TITAN'S AEOLIAN SALTATION THRESHOLD CONDITIONS: INITIAL RESULTS. K. D. Runyon[1], D. M. Burr[2], J. P. Emery[2], S. S. Sutton[2], E. V. Nield[2], J. K. Smith[3]. [1]JHU/APL, Laurel, MD, USA (kirby.runyon@jhuapl.edu), [2]University of Tennessee, Knoxville, TN, USA (dburr1@utk.edu), [3]Arizona State University and NASA/Ames, USA.

Introduction: *Titan:* Of the aeolian planets of Venus, Earth, Mars, Titan, and possibly Io and Pluto [1], Titan's sand dunes' orientation deviates the most from expected behavior. Landforms on Titan interpreted as seif (or longitudinal) dunes viewed in radar imply a sand-transporting wind direction of west-to-east [2,3] in contrast to atmospheric models predicting an east-to-west wind direction [4,5,6]. This conundrum could be explained if winds commonly blowing east-to-west are incapable of moving much sand (i.e., have sub-threshold wind speeds) but rare, strong winds blowing from west to east are capable of moving sand [4,7].

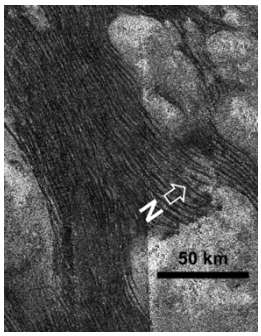

Figure 1. Seif dunes on Titan apparently formed in west-to-east winds despite more common—but perhaps weaker—east to west winds. Credit: NASA/JPL-Caltech/ASI, image PIA20710.

In addition to the uncertainty regarding Titan's wind regime, the properties of Titan's sand are not well constrained. The grains are likely composed of tholins with minor water ice [8], although the mechanism by which this organic sand is formed is still unknown. Recent experiments suggest that tholins at ambient temperatures have greater interparticle forces than one material used in threshold experiments [9].

Various evidence gives an age for Titan's atmosphere of only 300 Myr-1 Gyr old [10 & references therein]. Past higher or lower atmospheric pressures [e.g., 7] could have shaped the present landscape in unforeseen ways.

Aeolian Dynamics: The primary metric for describing the conditions for aeolian sand transport is friction wind speed, u^*, a shear speed at the fluid-surface boundary. The *threshold* friction wind speed u^*_t is the friction wind speed required to initiate movement. Dune formation requires movement by saltation, which is grain hopping induced by fluid mechanical and ballistic acceleration. The friction speed is not a physical speed but is related to the atmospheric density (ρ) and the shear stress (τ) acting on grains: $u^* = \sqrt{\frac{\tau}{\rho}}$. The first experimental investigation of threshold friction wind speeds for present-day Titan found values of $u^*_t \approx 0.05$-0.06 m/s [11]. Here, we provide new quantitative measurements for u^*_t for both present and paleo-climatic conditions (lower and higher atmospheric pressures) as derived from new experiments in a Titan-analog laboratory facility.

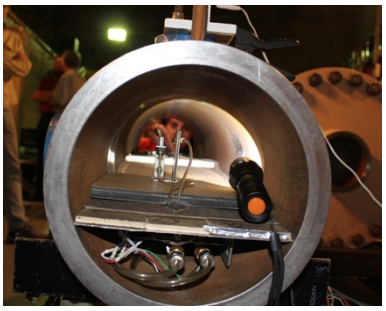

Figure 2. A view inside the test section of the TWT. The mount and tubing for the pitot tube are also visible. The internal diameter is 8 inches (20.32 cm). Crushed walnut shell forms the Titan sand simulant seen here.

Methods: As described in [12], the Titan Wind Tunnel (TWT) is an enclosed, pressurized wind tunnel designed to simulate the aeolian boundary conditions on Titan; it is the refurbished Venus Wind Tunnel (VWT) [13]. Because Titan gravity (1/7th Earth's gravity) cannot be duplicated in the lab, we rather achieve dynamic similarity for grain entrainment to Titan's conditions by matching a key dimensionless parameter between Earth and Titan: the particle Reynolds number, $Re^*_t = u^*_t D_p/\nu$, where D_p is the particle diameter and ν is the kinematic viscosity (molecular viscosity divided by the air density). Pressurizing the TWT to 12.5 bars achieves values of Re^*_t comparable to present-day Titan, which has a pressure of 1.5 bars. In aeolian dynamics, a sand grain's weight—not its mass—is the controlling factor in threshold conditions. Accordingly, we used crushed walnut shell as a Titan sand analog because it has the same weight as ice/tholin sand on Titan. Other granular materials of greater and lesser densities were also used as a basis of comparison and included basaltic sand, silica sand, and glass beads.

In order to observe the onset conditions of saltation, the fan motor speed was slowly increased with real-time human observers and video cameras noting various stages of grain movement. Movement progressed from "no movement," "twinkling/flurries" (when occasional grains moved), moving patches of sand, 50% (when it seemed 50% of the bed surface was in motion), and 100%. Burr et al. [11] defined threshold as 50% bed motion, consistent with prior Mars-analog experiments [14,15]. However, prior VWT experiments [13] defined threshold as the wind speed at which "groups of grains

began to saltate." To be more consistent with the VWT work, we present here the data from the "patches" category ("continuous grain motion but occurring over less than 50% of the bed; [11]) to define the saltation threshold. Although the definition of "moving patches" is somewhat subjective, our uncertainty analysis shows it to be relatively consistent between observers and between experimental runs. We recorded stages of motion for each bed 3-4 times, and included the variability in the wind speed at threshold in our uncertainty analysis.

Because u^* is not a physical speed, it must be calculated rather than measured by using the law-of-the-wall equation $u^* = \frac{\kappa U}{\ln \frac{z}{z_0}}$ where κ is the von Karman constant of 0.41, U is the free stream wind velocity above the boundary layer (measured by a fixed-position pitot tube), z is the measurement height above the ground (the height of a vertically-traversing pitot tube), and z_0 is the aerodynamic roughness height or the height above the ground at which wind is approximately still [e.g., 16]. The fixed-height pitot tube in the TWT recorded the free stream wind velocity U outside the turbulent boundary layer. We calculated z_0 from the wind speed profile measured by a variable-height pitot tube taken without grain motion.

The wind speed data at different heights were plotted as the natural logarithm of the height versus the wind speed. Fitting a log-linear curve to these data and noting the y-intercept yielded z_0. We conducted this procedure for each grain type at a variety of fan speeds. Depending on the material and grain size, our roughness heights ranged from ~1-9 μm with an average of 3.3 ± 1.1 μm.

To simulate paleo pressures on Titan, we ran TWT experiments over a range of pressures, from 1 to 20 bars.

Our last step is translating the TWT values to Titan values. As in Burr et al. [11], we scale the TWT results to Titan by the ratio of (u^*_{TWT}/ u^*_{Titan}), using the conversion factors (their Extended Data Figure 6) to convert TWT u^* values to Titan u^* values.

Results and Discussion: The threshold friction speeds for Titan are shown in Figure 3 along with the curves of Burr et al. [11]. Using the modified Iversen-White model [17] from Burr et al. [11], we report u^*_t = 0.06 ± 0.02 m/s for 125-250 μm grains of walnut, glass, and basaltic sand. Using the modified Shao and Lu [18] model, we report u^*_t = 0.055 ± 0.009 m/s. These values at 12.5 bar are essentially the same as measured previously by Burr et al. [11].

Figure 3 shows that u^*_t decreases with increasing pressure (wind at higher pressure moves sand more easily). If, given Titan's atmosphere's young age, the atmosphere is thinning with time, much of the aeolian geomorphology could be as old as Titan's atmosphere. If the atmosphere is rather thickening, then we would expect aeolian landforms to be younger.

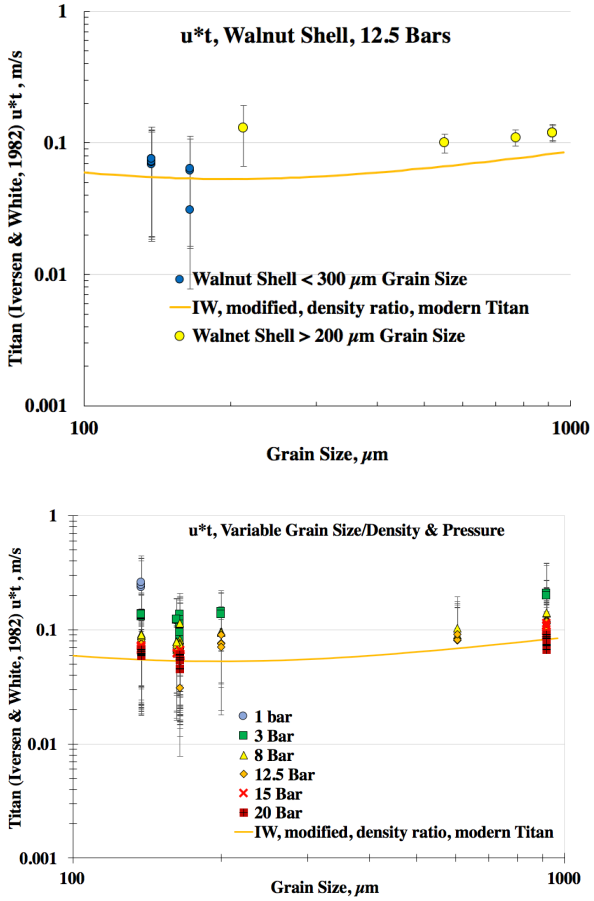

Figure 3. We converted the TWT u values to Titan u* values using the conversion ratios of Burr et al. [11] and compared them with the empirically modified Iversen and White [17] theoretical threshold friction curves. These theoretical curves are consistent with the experimental data.*

References: [1] Diniega, S., et al., (2017), Aeolian Research, http://dx.doi.org/10.1016/j.aeolia.2016.10.001. [2] Lorenz, R., et al., (2006), Science, doi:10.1126/science.1123257. [3] Lorenz, R., Radebaugh, J. (2009), GRL, doi:10.1029/2008GL036850. [4] Tokano, T. (2010), Aeolian Research, https://doi.org/10.1016/j.aeolia.2010.04.003. [5] Lebonnois, S. et al., (2014), ISBN 9780511973420. [6] Lora et al., (2015), https://doi.org/10.1016/j.icarus.2014.12.030. [7] Charnay, B., et al. (2015), Nature Geoscience, doi:10.1038/ngeo2406 [8] Barnes, J.W., et al. (2008), https://doi.org/10.1016/j.icarus.2007.12.006. [9] Yu, X., et al., (2017) JGR-Planets, doi:10.1002/2017JE005437. [10] Hörst, S.M., (2017), JGR-Planets, doi:10.1002/2016JE005240. [11] Burr, D., et al., (2015a), Nature, doi:10.1038/nature14088. [12] Burr, D., et al. (2015b), https://doi.org/10.1016/j.aeolia.2015.07.008. [13] Greeley, R., et al., 1984, Icarus, https://doi.org/10.1016/0019-1035(84)90013-7. [14] Greeley, R., et al., (1976), Geophysical Research Letters, doi:10.1029/GL003i008p00417. [15] Iversen, J.D., et al. (1976), Icarus, https://doi.org/10.1016/0019-1035(76)90140-8. [16] Bagnold, R.A., (1954), The Physics of Blown Sand and Desert Dunes, Dover Publications. [17] Iversen, J.D., White, B.R., (1982), Sedimentology, doi:10.1111/j.1365-3091.1982.tb01713.x. [18] Shao, Y., Lu, H., (2000), JGR-Atmospheres, doi:10.1029/2000JD900304.